*metals*

MDPI

*Article*

# The Influence of Coating and Adhesive Layers on the Mechanical Performance of Additively Manufactured Aluminum–Polymer Hybrid Joints

**Rielson Falck [1] and Sergio T. Amancio-Filho [2,*]**

[1] Helmholtz-Zentrum Hereon, Institut für Werkstoffmechanik, Solid State Materials Processing, 21502 Geesthacht, Germany
[2] BMK Endowed Professorship for Aviation, Institute of Materials Science, Joining and Forming, Graz University of Technology, Kopernikusgasse 24/1, 8010 Graz, Austria
* Correspondence: sergio.amancio@tugraz.at

**Abstract:** AddJoining technique has been recently introduced to produce metal–polymer composite hybrid layered structures. The methodology combines the principles of joining and polymeric additive manufacturing. This paper presents three AddJoining process-variants investigated and demonstrated for the material combination aluminum 2024-T3 and acrylonitrile butadiene styrene to form hybrid single lap joints. The microstructure and mechanical performance were assessed. The process variant using heating control showed the ultimate lap shear force of 1.2 ± 0.05 kN and displacement at a break of 1.21 ± 0.16 mm as a result of strong bonding formation at the interface of the hybrid joints. For instance, the other two process variants tested (with epoxy adhesive, and with thin-acrylonitrile butadiene styrene (ABS) coating layer applied on the metal) presented reduced mechanical performance in comparison to process variant using heating control, namely approximately 42% and 8.3%, respectively. The former had a mixed adhesive–cohesive failure due to the lower bonding performance between the adhesive and ABS printed layers. The latter displayed a slight decrease in force in comparison to heat-control specimens. This could be explained by the presence of micro-voids formed by solvent evaporation at the ABS coating layer during AddJoining.

**Keywords:** AddJoining; fused-filament fabrication (FFF); additive manufacturing; aluminum 2024-T3; ABS; metal–polymer



**Citation:** Falck, R.; Amancio-Filho, S.T. The Influence of Coating and Adhesive Layers on the Mechanical Performance of Additively Manufactured Aluminum–Polymer Hybrid Joints. *Metals* **2023**, *13*, 34. https://doi.org/10.3390/met13010034

Academic Editor: Guido Di Bella

Received: 15 November 2022
Revised: 14 December 2022
Accepted: 19 December 2022
Published: 23 December 2022



## 1. Introduction

The substitution of conventional metals by lightweight materials is a recent trend observed for structural applications. The driving forces in core industries (automotive and aerospace) are weight reduction and reliable mechanical performance. Thus, there is a need to search for the next generation of materials and innovative production technologies.

The application of multi-materials in a structure can bring essential benefits, but it is a challenge to combine dissimilar materials due to their differing physicochemical properties [1,2]. The essential characteristics of the development of structure is based on material, design, and manufacturing technique. Joining technologies and additive manufacturing techniques are techniques that can contribute to the successful integration of material, design, and manufacturing technique [3]. In fact, traditional joining methods can face technological limitations when joining dissimilar materials, for instance the combination of metals and composites. A good example is adhesive bonding, where the relatively long curing time of the adhesive is a significant drawback. In recent years, new joining techniques have been investigated to develop hybrid structures to overcome the limitations of traditional joining methods [2,4]. These include novel energy efficient friction-based techniques [5], such as friction riveting [6–8], friction spot joining [9–12], ultrasonic welding [13,14] and ultrasonic joining [15–17]. Other fusion-based joining technologies, such

as laser joining [18,19], resistance spot joining [20], injection clinching joining [21–23], and induction-heated joining [24,25], have also proven to be adequate to produce hybrid joints.

Currently, the manufacture of metal–polymer layered parts is very demanding; usually long processing cycles are required to cure the thermoset-based resin, such as in epoxy-based fiber-metal laminates (FML) [26]. Cortés and Cantwell [27] investigated emerging thermoplastic-based FML (T-FML), such as carbon-fiber reinforced PEEK/Ti. An advantage of T-FMLs is associated with its short thermoforming cycles. Although, there are challenges on the automation and ability to make complex parts to manufacture current FML and T-FML materials. The scenario is similar to traditional metal-composite layered structures, such as those produced by co-bonding and co-curing. A recent alternative approach to mitigate or overcome such state-of-the-art challenges involves automating the FML manufacture by additive manufacturing (AM); besides AM normally improve the freedom in complex part designing [28]. Recently, Janssen, Peters and Brecher [29] reported an AM approach to join hybrid parts tailor-making carbon-fiber-reinforced polyamide-6 and 3D-printed polyamide-12 parts. Lately, an increased interest in the field of AM has promoted the flexibility to produce complex geometric parts with net-shaped and mechanical functionalities, e.g., in sandwich structures with AM honeycomb cores [30,31].

Falck et al. [32] recently introduced AddJoining technology as an alternative method to produce metal–polymer (composite) layered structures based on the principles of joining and the polymeric AM. In the early phase of this technology, it is necessary to understand the adhesion forces and interactions between the metal and the polymer. In previous publications [32,33], the authors discussed the influence of process parameters on the mechanical behavior of hybrid joints. More recently, Belei, Pommer and Amancio-Filho [34] investigated the use of sandblasted, rolled Ti-6Al-4V substrates and short carbon fiber-reinforced polyamide (PA-CF). The authors used simple Machine Learning algorithms—i.e., linear and polynomial regressions—to evaluate the influence of layer height, printing speed and printing bed temperature for the coating layer of unreinforced polyamide 6 on the ultimate single-lap shear strength (ULSS) of the Add-joints. The linear model achieved a good accuracy, with a R2 = 0.76. The authors concluded that the ULSS was directly proportional to the coating layer height, the latter being strongly dependent both on the printing speed and on the input layer height. Not only wrought metals were hybridized by means of AddJoining. Oliveira et al. [35] showed the feasibility of creating sub-millimetric textures on the surface laser-powder-bed-fusion 3D-printed AlSi10Mg additively manufactured alloys. They used submillimeter-sized mushroom-shaped structures which allowed for good micro-mechanical interlocking with add-joined polycarbonate. PC/AlSi10Mg hybrid addjoints with excellent lap-shear strength of $10.8 \pm 0.6$ MPa could be achieved.

This study enables the first insights into the understanding the available AddJoining process variants. Two well-established materials were selected for this study: aluminum alloy 2024-T3 and acrylonitrile butadiene styrene (ABS). The current work aims to evaluate the influence of different AddJoining process variants—i.e., (a) use of epoxy-based adhesive, (b) with heating control and (c) with thin-ABS-coated metal—on the mechanical behavior and microstructure of hybrid joints.

## 2. Fundamentals of the AddJoining Process

AddJoining is inspired by AM and joining technology principles, where the new technique uses polymer 3D printing, e.g., fused filament fabrication (FFF). In the AddJoining method, FFF is applied to form the polymeric part. Hence, the parts can be produced with complex geometries by depositing extruded material layer by layer on a substrate. This manufacturing technique is divided into three mains steps (Figure 1) [32]. Prior to starting to produce the metal–polymer hybrid part, AddJoining begins by slicing a 3D CAD data into layers. The first phase starts by fixing the metallic substrate on the build platform (Figure 1a). Subsequently, the polymer material is uncoiled slowly and guided to the extrusion head, where the resistive heated part is located closer to the nozzle. This is heated to high temperatures (above glass transition temperature or melting temperature)

to decrease material viscosity. At this stage, the softened or molten material flows smoothly through the extrusion nozzle, where the polymer material is deposited to form a full layer on top of the metal substrate (Figure 1b). Following each sequence, the building platform is lowered down in Z-direction by the thickness of one layer, while the extrusion head moves in X-Y plane, e.g., a horizontal plane. The process continues by adding polymer layers on top of the previously consolidated polymer, until the final thickness of the polymeric part is achieved (Figure 1c). The last stage of the process is by removing the metal–polymer layered joint from the building platform (Figure 1d). Additional post-printing steps (e.g., thermomechanical treatment), such as hot isostatic pressing, may be applied to eliminate intrinsic voids in the layered component. Note that post-processing was not considered in this work. However, this technique is usually used to produce a homogeneous and defect-free material for 3D-printed parts [36].

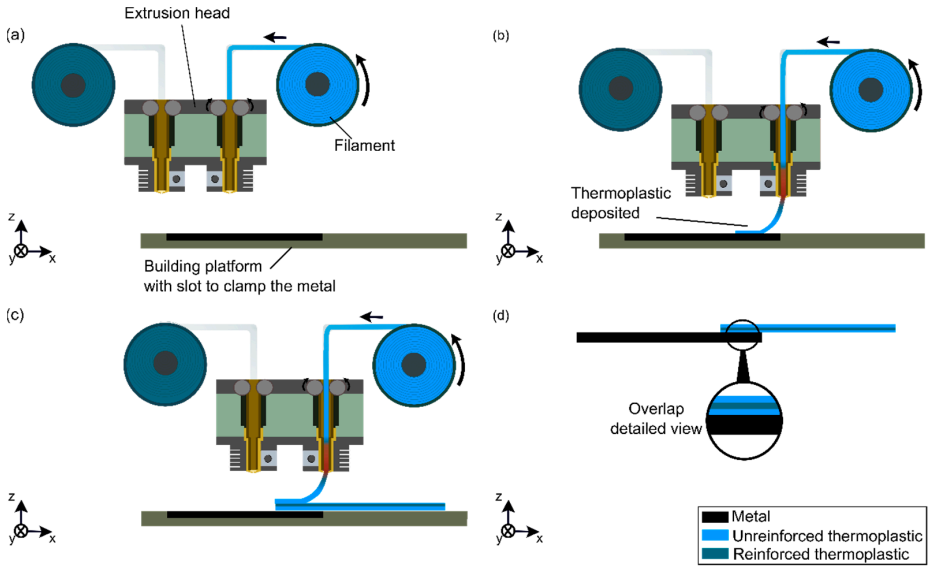


**Figure 1.** Schematic representation of the AddJoining process for layered metal–polymer composite hybrid structures: (**a**) initial setup, (**b**) deposition of the first polymer layer on the metal substrate, (**c**) deposition of the subsequent polymer layers, (**d**) final layered metal–polymer hybrid structure. Reprinted with permission from ref. [32]. Copyright 2022 Elsevier.

## 3. Materials and Methods

### *3.1. Base Materials*

In this exploratory study, the base materials used were two-millimeter-thick aluminum alloy 2024-T3 rolled sheets (Costellium, Paris, France) with the following nominal chemical composition in weight percent [37]: ≤0.1% Cr; 3.8–4.9% Cu; ≤0.5% Fe; 1.2–1.8% Mg; 0.3–0.9% Mn; ≤0.5% Si; ≤0.15% Ti; ≤0.25% Zn and 90.7–94.7% Al. The metal alloy has excellent mechanical properties and applicability in the transportation industry. Hence, such material belongs to the 2xxx series of precipitation hardening aluminum alloy, where copper and magnesium are the major alloying elements. Table 1 shows the physical and mechanical properties of the aluminum 2024-T3.

**Table 1.** Primary physical and mechanical properties of aluminum 2024-T3 at room temperature [38].

| Coeff. of Thermal Expansion (μm/m-°C) | Thermal Conductivity (W/m-K) | Melting Temperature (°C) | Elastic Modulus (GPa) | Tensile Strength (MPa) |
|---|---|---|---|---|
| 24.7 | 121 | 500–638 | 72 | 480 |

As a polymeric part, an unreinforced thermoplastic was selected and supplied by VShaper, Rzeszów, Poland, in a spool with a filament 1.75 mm in diameter. ABS is an

amorphous thermoplastic, which is a terpolymer with a glass transition temperature of 94 °C [39–41]. Table 2 depicts some of the physical and mechanical properties of ABS. This polymer is widely used for engineering applications, such as to fulfill impact resistance, strength, and stiffness [42,43].

**Table 2.** Primary physical and mechanical properties of ABS at room temperature [39–41].

| Coeff. of Thermal Expansion (μm/m-°C) | Thermal Conductivity (W/m-K) | Glass Transition Temperature (°C) | Elastic Modulus (GPa) | Tensile Strength (MPa) |
|---|---|---|---|---|
| 10.1 | 0.21 | 94 | 2.4 | 26 |

### *3.2. Manufacturing Procedure*

Prior to manufacturing of the AddJoining hybrid joints, the surface of the metal was sand-blasted with corundum ($Al_2O_3$) with particle size ranging from 100 to 150 μm (WIWOX Surface Systems, Erkrath, Germany) using a pressure of six bar. The samples were cleaned with pressurized air and immersed cleansed in ethanol ultrasonic bath for three minutes. The sand-blasting treatment helps to create crevices in the surface of the metal, which will act as micro-mechanical anchoring sites for the polymer after consolidation of the coating layer [33,34]. Currently, AddJoining was reported to have five controllable manufacturing parameters, with four of these depending on the 3D printer and process variant selected [33]. In this study a commercial VShaper PRO (VShaper, Rzeszów, Poland) fused filament fabrication (FFF) 3D printer was utilized to manufacture the hybrid Add-joints. Four controllable parameters were used: printing temperature (PT: 250 °C), road thickness (RT: 0.2 mm), deposition speed (DS: 40 mm/s), and number of contours (NC: 2). With the defined controllable parameters, the total manufacturing time per sample is 55 min. Moreover, road angle at [−45°, 45°] (i.e., deposition directions alternately for different layers in −45° and 45°) and building surface temperature at 115 °C were kept constant. In this investigation a simple one-factor-at-a-time, OFAT design of experiment (DoE) was carried out to obtain the initial understanding of the AddJoining technique for this combination of materials. The following joining parameters and their ranges were investigated: PT: 230–280 °C; RT: 0.1–0.3 mm; DS: 20–60 mm/s and NC: 2–22. A more advanced DoE is required to fully maximize mechanical strength of each process variant. However, this is out of the scope of this manuscript.

The first variant of the process was tested using the epoxy-based adhesive DP490 3M, Saint Paul, MN, USA) applied on sandblasted metal parts (average thickness of uncured adhesive of 200 μm). Following that the ABS part was directly add-joined to the metal with adhesive before curing. Finally, curing procedure was applied following the supplier procedure in two cycles, whereby the adhesive hybrid joints were kept one day at room temperature and subjected to the second cycle in the air-circulating oven Nabertherm TR60 (Nabertherm, Lilienthal, Germany) at 80 °C for 1 h. The second process variant was tested using a heating-control system, where a first layer of ABS was deposited on the surface of the sand-blasted aluminum part by 3D-printing/indirect heating as follows: (1) printing a stand-alone layer of ABS (13 mm × 26 mm × 0.2 mm); (2) heating the aluminum part with the stand-alone ABS printed coating layer using an external hot plate at 250 °C for one minute (to remelt and homogenize the stand-alone printed ABS layer); (3) allowing a two-minute consolidation time for ABS coating. The third variant consists of forming the thin ABS coating layer in the sand-blasted metal using an adapted dip-coating method. To perform the coating, the ABS filament was dissolved in pure acetone at room temperature for 24 h to form a 15 wt.% ABS solution. A homogeneous coating was manually applied with a customized gauge-tool to support uniform spreading and to ensure a constant coating thickness (60 μm) on the aluminum surface [33]. The samples were subsequently dried in the horizontal position for five minutes at room temperature to allow for hardening of the deposited coating. For each process variant, three replicates of the lap shear test specimens were produced and tested.

### *3.3. Microstructure and Mechanical Analysis*

For each process variant, the microstructure and mechanical performance were evaluated. To analyze the microstructure of the hybrid joints, a cross-section of the joints was cut from the overlapped zone (specimen size approximately 12.5 mm × 12.5 mm × 4 mm) longitudinally to the length of the lap-shear testing specimens (Figure 2). This was then mounted, ground, and polished, following standard methods to obtain a smooth surface and examined by reflected-light optical microscopy (RLOM) using a Leica DM IRM optical microscope (Leica Microsystems, Wetzlar, Germany). The hybrid joints were evaluated under quasi-static loading to assess the mechanical performance. Based on ASTM D3163-01, the single-lap shear test was performed in a Zwick/Roell 1478 universal testing machine with 100 kN force cell (Zwick/Roell, Ulm, Germany) at room temperature with a transverse speed of 1.27 mm/min. The final AddJoining lap joints had the specimen geometry of 101.6 mm × 25.5 mm × 2 mm with an overlap area of 12.5 mm × 25.5 mm (Figure 2).

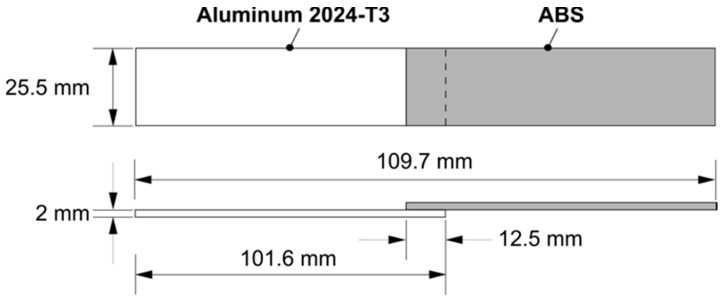


**Figure 2.** Schematic of lap shear testing specimen geometry for the AddJoining hybrid joints.

## 4. Results and Discussion

The quasi-static mechanical performance of AddJoints is shown in Figure 3. The stiffness among the process variants are similar (Figure 3a). The force-displacement curves of the different process variants showed a linear elastic behavior and similarity on the stiffness prior to failure. The variant using adhesive showed limited displacement at break (DaB: 0.67 ± 0.04 mm) representing the low-ductility of the adhesive. In contrast to the process variant using heating control, the displacement at break was 79% higher than the variant using adhesive (DaB: 1.21 ± 0.16 mm). For the variant three (using thin-coating layer), the displacement at break was 67% higher than the variant using adhesive (DaB: 1.12 ± 0.06 mm). Figure 3b compares the average ultimate lap shear force (ULSF) obtained from force-displacement curves. Process variant two (the heating-control variant) displayed an average ULSF of 1.2 ± 0.05 kN. Hence, process variant one and three showed lower mechanical performance compared to the heating control variant, about 42% (ULSF: 0.7 ± 0.1 kN) and 8.3% (ULSF: 1.1 ± 0.06 kN), respectively.

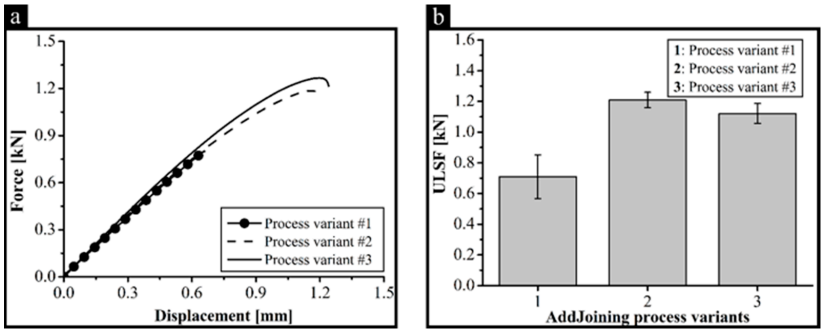


**Figure 3.** Mechanical performance of the AddJoining process variants: (**a**) representative force-displacement curves for process variant one (with adhesive), variant two (with heating control) and variant three (with thin-coating layer). (**b**) average ULSF for each process variant.

For process variant one (epoxy adhesive), the poor mechanical performance using commercial adhesive can be explained on one hand by the inherent difficulties of bonding thermoplastics to other polymers or metals because of their low surface tension [44,45]; thermoplastic adherends usually requires specific surface treatments applied by physical (e.g., peel-ply, grit blasting) or chemical (e.g., plasma surface treatment) means to produce high performance adhesively bonded joints [2,45–49], which were not applied in the tested polymeric coatings used in this work. On the other hand, a reduced final average thickness of 32 $\pm$ 2 µm of the epoxy adhesive in the hybrid joints was observed (Figure 4a). During the printing of the ABS part, the extruder head movement removed part of the uncured adhesive from the metallic part's surface due to the contact with the 3D-printing nozzle. According to Boutar et al. [50], the ideal bond line thickness using structural adhesive is in average between 200 µm to 500 µm. The authors reported that interface stresses are higher with thin adhesive bond line thicknesses, which may reduce the carry load capability of the adhesive [50,51]. For process variants two and three, Figure 4b,c, respectively, a close contact could be achieved between the coating layer and the surface of the aluminum and between the deposited polymer and coating layer. For process variant three, the presence of voids in the ABS coating is believed to be related to the evaporation of residual acetone from the coating solution during the AddJoining printing stage. This is a reasonable assumption, considering that PT = 250 °C and pure acetone has a boiling point of 56 °C [52]. Moreover, such phenomenon was not present in the process variant two (heating-control) specimens; this suggests the flaws in Figure 4c are not thermal degradation gases. Mendelson [53] correlated the melt viscosity dependence of ABS with temperature. The author reported that a variation in temperature reduced the melt viscosity up to 50% (4600 Pa-s (230 °C) and 2500 Pa-s (260 °C)), where the bonding between the layers is activated because the consolidation process is thermally driven by the polymer viscous flow process [54]. Keeping the temperature above the glass transition temperature ($T_g$ = 94 °C [33,39,55]) in AddJoining helps to ensure that there would be good bonding between successively deposited layers, explaining the absence of defects and the presence of smooth welding line for process-variant two specimens. Therefore, for both variant two and three specimens, the primary bonding mechanisms between the printed layers are by thermal fusion and interlayer bonding (i.e., intermolecular diffusion), whereby pores were formed by the evaporation of residual solvent molecules in the applied ABS coating.

Figure 5 illustrates the failure type of the process variant (1) with adhesive layer, (2) ABS coating obtained with heating control and (3) ABS coating achieved with ABS solution. There are clearly three different failure types among the AddJoining process variants. These are a result of the different bonding mechanisms among the process variants. Figure 5a illustrates the joint fracture surface observed for process variant one. Due to the limited bonding performance between the 3D-printed ABS and adhesive (black areas) in the surface of the aluminum 2024-T3 part, failure took place mostly at the interface between adhesive and add-joined ABS; however, one may observe a few adhesive-rich areas in the ABS part (see arrows in Figure 5a). Therefore, specimens of process variant one presented an adhesive–cohesive failure [56,57].

On the contrary, the strong bonding formation obtained with the heating-control approach (process variant two) resulted in specimens failing in the ABS printed part. Stock-break failure [58] occurred by tensile failure outside of the overlap joint area across the width of the 3D-printed ABS (Figure 5b). This typical failure is rarely reported for hybrid single-lap joints, suggesting the presence of a strong interface between the adherends (i.e., aluminum 2024-T3 and 3D-printed ABS). When single-lap joints have strongly joined overlap areas, the failure is driven to possible areas with peak stress concentrations, which are located at the free edges of the lap joint [2,59]. In this work AddJoining uses the FFF process as the main backbone to produce the hybrid joints. A well-known current limitation of the FFF process is the presence of intrinsic voids related to air gaps during printing [55,60–63]. The voids act as stress concentrators, contributing to anisotropy of the mechanical properties. Thus, for the process variant using heating control, the strong

interface drives the failure to the 3D-printed part to fail at lower stresses—in comparison with injection molded ABS parts [64]—due to FDM-process-related intrinsic voids.

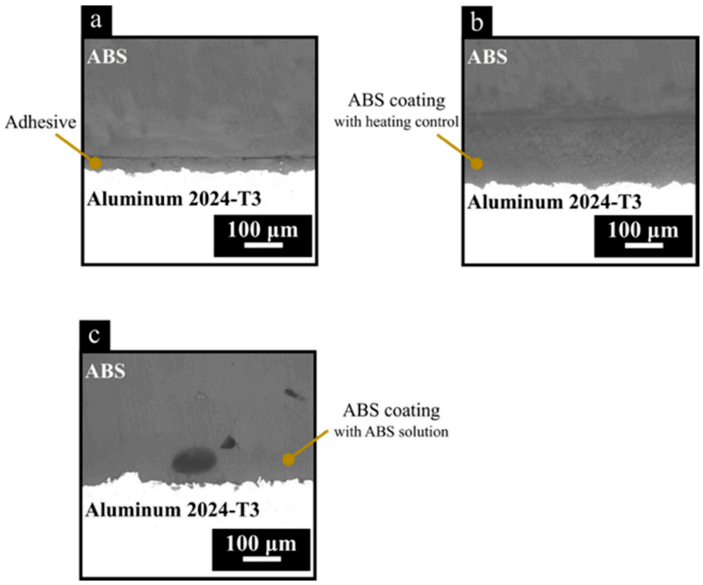


**Figure 4.** Microstructure of overlap joints from the investigated AddJoining process variants: (**a**) process variant one (with adhesive), (**b**) variant two (with heating control) and (**c**) variant three (with thin-coating layer). Specimens for microscopy were cut from the overlap zone in the longitudinal direction from lap-shear testing specimens, Figure 2.

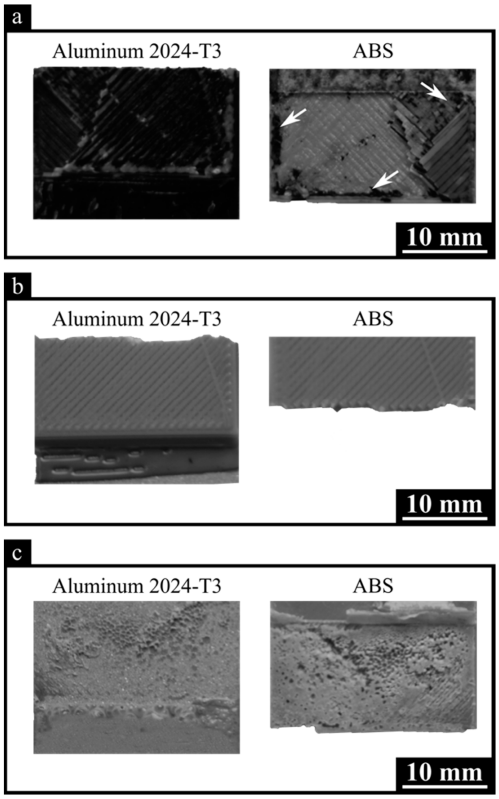


**Figure 5.** Fracture surface from the mechanically tested AddJoining hybrid joints for (**a**) process variant one (with adhesive), (**b**) variant two (with heating control) and (**c**) variant three (with thin-coating layer). Figures show the whole overlap area of hybrid joints after mechanical testing. The direction of the load application during lap-shear testing is aligned from the bottom to the top of the figures.

Figure 5c shows a dominant adhesive failure regime, with a very thin layer of ABS coating remaining attached to the metallic surface. Moreover, one can see the presence of voids (tiny bubbles) in the ABS coating owing to the evaporation of residual acetone during AddJoining. Nevertheless, at the microscopic level, the presence of voids in the ABS coating does not appear to sufficiently affect the overall mechanical performance of the AddJoining hybrid joints. This may be associated to two factors: (a) the coating deposition was very effective and good micro-mechanical interlocking was achieved between the coated metal substrate and the 3D-printed polymer, and (b) good bonding between the coating and printed ABS (i.e., good intermolecular diffusion) was achieved during AddJoining. Further in-progress investigations will help to confirm these assumptions regarding the micro-mechanisms of failure in AddJoining specimens.

## 5. Conclusions

The AddJoining technique has been successfully applied to combine aluminum 2024-T3 and acrylonitrile butadiene styrene to form hybrid joints. Furthermore, the quasi-static properties of different AddJoining process variants one (with adhesive), variant two (with heating control) and variant three (with thin-coating layer) were evaluated.

Process variant one (with epoxy-based adhesive) and three showed lower mechanical performance compared to the heating control variant, 42% (ULSF: 0.7 $\pm$ 0.1 kN) and 7% (ULSF: 1.1 $\pm$ 0.1 kN), respectively. The lower mechanical performance for hybrid joints using commercial adhesive is, on one hand an indication of the low surface tension from the thermoplastic (i.e., limited adhesion forces), and on the other hand due to the decrease from 200 μm (originally applied adhesive layer) to 32 $\pm$ 2 μm, whereby the uncured adhesive was partially removed due to the contact of the nozzle on the extruder head during the printing of the first layers. As known from the literature, adhesive layers in bonded joints should have a thickness between 200–500 μm to avoid high interface stresses, reducing the carry load capability. For the process variant three (with thin-coating layer), the presence of voids in the ABS coating was visible, caused by the evaporation of residual acetone. Compared to process two (with heating control) specimens, at the microscopic level, micro-voids in process-variant-three specimens were not sufficiently decisive to strongly decrease the overall mechanical performance of the AddJoining hybrid joints. This is mainly due to the good intermolecular diffusion between ABS-coating and printed ABS. As voids were not visually found present in process variant two (heat-control) and similar intermolecular diffusion (i.e., thermal fusion and interlayer bonding) between coating and printed part took place, these specimens presented the highest quasi-static mechanical performance of 1.20 $\pm$ 0.05 kN in this study.

All in all, the results of this study opened up the possibility to further understand and advance the AddJoining technique for future polymer–metal hybrid structures. In this study, the heating control process variant has been shown to be the preferred strategy to improve the mechanical performance and reproducibility of the process. The application of a heating control is believed to contribute to increasing the build temperature above the polymer glass transition temperature, thereby supporting the bond formation between the 3D printed layers by macromolecular autohesion between polymeric printed layers and better wetting and spreading at the aluminium surface. Intensive ongoing work—to be published in a separate manuscript—on the correlation between processing, microstructure and mechanical performance at the coupon level will allow for process scaling-up to produce future layered metal–polymer structures.

**Author Contributions:** Conceptualization, R.F. and S.T.A.-F.; formal analysis, R.F.; investigation, R.F.; methodology, R.F. and S.T.A.-F.; supervision, S.T.A.-F.; writing—original draft preparation, R.F.; writing—review and editing, R.F. and S.T.A.-F. All authors have read and agreed to the published version of the manuscript.

**Funding:** R. Falck would like to thank Conselho Nacional de Pesquisa—CNPq, Brazil for financial support (grant number: 200674/2015-3). S.T. Amancio-Filho would like to acknowledge the Austrian

aviation program "TAKE-OFF" and the Austrian Ministry for Climate Action, Environment, Energy, Mobility, Innovation and Technology, BMK (Austria), grant number 852796, 2018. Open Access Funding by the Graz University of Technology.

**Data Availability Statement:** The data presented in this study are available on request from the corresponding author.

**Acknowledgments:** The authors would like to acknowledge Open Access Funding by the Graz University of Technology.

**Conflicts of Interest:** The authors declare no conflict of interest.

## References

1. Mallick, P.K. Joining for Lightweight Vehicles. In *Materials, Design and Manufacturing for Lightweight Vehicles*; Woodhead Publishing Series in Composites Science and Engineering; Mallick, P.K., Ed.; Woodhead Publishing: Sawston, UK, 2010; pp. 275–308. ISBN 978-1-84569-463-0.
2. Amancio-Filho, S.T.; Blaga, L.A. *Joining of Polymer—Metal Hybrid Structures: Principles and Applications*; John Wiley & Sons, Inc.: Hoboken, NJ, USA, 2018; ISBN 9781119429807.
3. Goede, M.; Stehlin, M.; Rafflenbeul, L.; Kopp, G.; Beeh, E. Super Light Car—Lightweight Construction Thanks to a Multi-Material Design and Function Integration. *Eur. Transp. Res. Rev.* **2009**, *1*, 5–10. [CrossRef]
4. Amancio-filho, S.T. Metal-Polymer Multi-Material Structures and Manufacturing Techniques in Transportation. In *Metal-Polymer Multi-Material Structures and Manufacturing Techniques in Transportation*; MDPI Books: Basel, Switzerland, 2020. [CrossRef]
5. Lambiase, F.; Balle, F.; Blaga, L.A.; Liu, F.; Amancio-Filho, S.T. Friction-Based Processes for Hybrid Multi-Material Joining. *Compos. Struct.* **2021**, *266*, 1138. [CrossRef]
6. Altmeyer, J.; Suhuddin, U.F.H.; Dos Santos, J.F.; Amancio-Filho, S.T. Microstructure and Mechanical Performance of Metal-Composite Hybrid Joints Produced by FricRiveting. *Compos. Part B Eng.* **2015**, *81*, 130–140. [CrossRef]
7. Amancio-Filho, S.T.; dos Santos, J.F. FricRiveting: A New Technique for Joining Thermoplastics to Lightweight Alloys. In Proceedings of the 66th Annual Technical Conference of the Society of Plastics Engineers 2008, Milwaukee, WI, USA, 4–8 May 2008; pp. 841–845.
8. Borba, N.Z.; Kötter, B.; Fiedler, B.; dos Santos, J.F.; Amancio-Filho, S.T. Mechanical Integrity of Friction-Riveted Joints for Aircraft Applications. *Compos. Struct.* **2020**, *232*, 111542. [CrossRef]
9. Goushegir, S.M.; Santos, J.F.; Amancio-Filho, S.T. Influence of Process Parameters on Mechanical Performance and Bonding Area of AA2024/Carbon-Fiber-Reinforced Poly (Phenylene Sulfide) Friction Spot Single Lap Joints. *Mater. Des.* **2015**, *83*, 431–442. [CrossRef]
10. Manente André, N.; Goushegir, S.M.; Scharnagl, N.; dos Santos, J.F.; Canto, L.B.; Amancio-Filho, S.T. Composite Surface Pre-Treatments: Improvement on Adhesion Mechanisms and Mechanical Performance of Metal–Composite Friction Spot Joints with Additional Film Interlayer. *J. Adhes.* **2018**, *94*, 723–742. [CrossRef]
11. Goushegir, S.M.; dos Santos, J.F.; Amancio-Filho, S.T. Influence of Aluminum Surface Pre-Treatments on the Bonding Mechanisms and Mechanical Performance of Metal-Composite Single-Lap Joints. *Weld. World* **2017**, *61*, 1099–1115. [CrossRef]
12. André, N.M.; dos Santos, J.F.; Amancio-Filho, S.T. Evaluation of Joint Formation and Mechanical Performance of the AA7075-T6/CFRP Spot Joints Produced by Frictional Heat. *Materials* **2019**, *12*, 891. [CrossRef]
13. Balle, F.; Wagner, G.; Eifler, D. Ultrasonic Metal Welding of Aluminium Sheets to Carbon Fibre Reinforced Thermoplastic Composites. *Adv. Eng. Mater.* **2009**, *11*, 35–39. [CrossRef]
14. Balle, F.; Wagner, G.; Eifler, D. Ultrasonic Spot Welding of Aluminum Sheet/Carbon Fiber Reinforced Polymer—Joints. *Mater. Werkst.* **2007**, *38*, 934–938. [CrossRef]
15. Feistauer, E.E.; Guimarães, R.P.M.; Ebel, T.; Dos Santos, J.F.; Amancio-Filho, S.T. Ultrasonic Joining: A Novel Direct-Assembly Technique for Metal-Composite Hybrid Structures. *Mater. Lett.* **2016**, *170*, 1–4. [CrossRef]
16. Carvalho, W.S.; Amancio-Filho, S.T. On the feasibility of joining additively-manufactured 316L stainless steel and poly-ether-ether-ketone by ultrasonic energy. *Add. Manufac. Lett.* **2022**, *3*, 100098. [CrossRef]
17. Feistauer, E.E.; dos Santos, J.F.; Amancio-Filho, S.T. An Investigation of the Ultrasonic Joining Process Parameters Effect on the Mechanical Properties of Metal-Composite Hybrid Joints. *Weld. World* **2020**, *64*, 1481–1495. [CrossRef]
18. Schricker, K.; Alhomsi, M.; Bergmann, J.P. Thermal Efficiency in Laser-Assisted Joining of Polymer–Metal Composites. *Materials* **2020**, *13*, 4875. [CrossRef] [PubMed]
19. Schricker, K.; Bergmann, J.P.; Hopfeld, M.; Spieß, L. Effect of Thermoplastic Morphology on Mechanical Properties in Laser-Assisted Joining of Polyamide 6 with Aluminum. *Weld. World* **2021**, *65*, 699–711. [CrossRef]
20. Szallies, K.; Bielenin, M.; Schricker, K.; Bergmann, J.P.; Neudel, C. Single-Side Resistance Spot Joining of Polymer-Metal Hybrid Structures. *Weld. World* **2019**, *63*, 1145–1152. [CrossRef]
21. Abibe, A.B.; Sônego, M.; Santos, J.F.; Canto, L.B.; Amancio-Filho, S.T. On the Feasibility of a Friction-Based Staking Joining Method for Polymer—Metal Hybrid Structures. *Mater. Des.* **2016**, *92*, 632–642. [CrossRef]

22. Abibe, A.B.; Amancio-Filho, S.T.; dos Santos, J.F.; Hage, E.H., Jr. Mechanical and Failure Behaviour of Hybrid Polymer—Metal Staked Joints. *Mater. Des.* **2013**, *46*, 338–347. [CrossRef]
23. Sônego, M.; Abibe, A.B.; Canevarolo, S.V.; Bettini, S.H.P.; Dos Santos, J.F.; Canto, L.B.; Amancio-Filho, S.T. Thermomechanical Degradation of Polyetherimide (PEI) by Friction-Based Joining and the Effects on Quasi-Static Mechanical Strength of Hybrid Joints. *Int. Polym. Process.* **2019**, *34*, 100–110. [CrossRef]
24. Mitschang, P.; Velthuis, R.; Emrich, S.; Kopnarski, M. Induction Heated Joining of Aluminum and Carbon Fiber Reinforced Nylon 66. *J. Thermoplast. Compos. Mater.* **2009**, *22*, 767–801. [CrossRef]
25. Weidmann, S.; Hümbert, M.; Mitschang, P. Suitability of Thickness Change as Process Control Parameter for Induction Welding of Steel/TP-FRPC Joints. *Adv. Manuf. Polym. Compos. Sci.* **2019**, *5*, 55–68. [CrossRef]
26. Vlot, A.; Gunnink, J.W. *Fibre Metal Laminates: An Introduction*; Springer Science: Berlin/Heidelberg, Germany, 2011.
27. Cortés, P.; Cantwell, W.J. The Prediction of Tensile Failure in Titanium-Based Thermoplastic Fibre-Metal Laminates. *Compos. Sci. Technol.* **2006**, *66*, 2306–2316. [CrossRef]
28. Steve Upcraft; Richard Fletcher the Rapid Prototyping Technologies. *Assem. Autom.* **2003**, *23*, 318–330. [CrossRef]
29. Janssen, H.; Peters, T.; Brecher, C. Efficient Production of Tailored Structural Thermoplastic Composite Parts by Combining Tape Placement and 3d Printing. *Procedia CIRP* **2017**, *66*, 91–95. [CrossRef]
30. Türk, D.; Kussmaul, R.; Zogg, M.; Klahn, C.; Spierings, A.; Ermanni, P.; Meboldt, M. *Additive Manufacturing with Composites for Integrated Aircraft Structures*; SAMPE: Long Beach, CA, USA, 2016.
31. Riss, F.; Schilp, J.; Reinhart, G. Load-Dependent Optimization of Honeycombs for Sandwich Components-New Possibilities by Using Additive Layer Manufacturing. *Phys. Procedia* **2014**, *56*, 327–335. [CrossRef]
32. Falck, R.; Goushegir, S.M.; dos Santos, J.F.; Amancio-Filho, S.T. AddJoining: A Novel Additive Manufacturing Approach for Layered Metal-Polymer Hybrid Structures. *Mater. Lett.* **2018**, *217*, 211–214. [CrossRef]
33. Falck, R.; dos Santos, J.; Amancio-Filho, S.T. Microstructure and Mechanical Performance of Additively Manufactured Aluminum 2024-T3/Acrylonitrile Butadiene Styrene Hybrid Joints Using an AddJoining Technique. *Materials* **2019**, *12*, 864. [CrossRef]
34. Belei, C.; Pommer, R.; Amancio-Filho, S.T. Optimization of additive manufacturing for the production of short carbon fiber-reinforced polyamide/Ti-6Al-4V hybrid parts. *Mater. Design* **2022**, *219*, 110776. [CrossRef]
35. Oliveira, G.H.M.; Belei, C.; Carvalho, W.S.; Canto, L.B.; Amancio-Filho, S.T. On the fully additive manufacturing of PC/AlSi10Mg hybrid structures. *Mater. Lett.* **2023**, *330*, 133378. [CrossRef]
36. Jarvela, P.; Heponen, V.P.; Jarvela, P. Hot Isostatic Pressing of Plastics. *Polym. Commun.* **1986**, *27*, 180–181.
37. *Aluminum AA2024-T3 Technical Datasheet*; Constellium France: Paris, France, 2012.
38. Davis, J.R. *Metals Handbook*; ASM International: Almere, The Netherlands, 1998; p. 2571.
39. Sun, Q.; Rizvi, G.M.; Bellehumeur, C.T.; Gu, P. Effect of Processing Conditions on the Bonding Quality of FDM Polymer Filaments. *Rapid Prototyp. J.* **2008**, *14*, 72–80. [CrossRef]
40. Agarwala, M.K.; Jamalabad, V.R.; Langrana, N.A.; Safari, A.; Whalenstephen, P.J.; Danforth, C. Structural Quality of Parts Processed by Fused Deposition. *Rapid Prototyp. J.* **1996**, *2*, 4–19. [CrossRef]
41. *Stratasys ABS-ESD7—Production Grade Thermoplastic for Fortus 3D Production Systems*; Stratasys: Austin, TX, USA, 2021; pp. 6–7.
42. Uddandapu, P.K. Impact Analysis on Car Bumper by Varying Speeds Using Materials ABS Plastic and Poly Ether Imide by Finite Element Analysis Software Solid Works. *Int. J. Mod. Eng. Res.* **2013**, *3*, 391–395.
43. Froelich, D.; Maris, E.; Haoues, N.; Chemineau, L.; Renard, H.; Abraham, F.; Lassartesses, R. State of the Art of Plastic Sorting and Recycling: Feedback to Vehicle Design. *Miner. Eng.* **2007**, *20*, 902–912. [CrossRef]
44. Schonhorn, H.; Hansen, R.H. Surface Treatment of Polymers for Adhesive Bonding. *J. Appl. Polym. Sci.* **1967**, *11*, 1461–1474. [CrossRef]
45. Iqbal, H.M.S.; Bhowmik, S.; Benedictus, R. Surface Modification of High Performance Polymers by Atmospheric Pressure Plasma and Failure Mechanism of Adhesive Bonded Joints. *Int. J. Adhes. Adhes.* **2010**, *30*, 418–424. [CrossRef]
46. Ochoa-Putman, C.; Vaidya, U.K. Mechanisms of Interfacial Adhesion in Metal-Polymer Composites—Effect of Chemical Treatment. *Compos. Part A Appl. Sci. Manuf.* **2011**, *42*, 906–915. [CrossRef]
47. Rotheiser, J. *Joining of Plastics: Handbook for Designers and Engineers*; Hanser: Munich, Germany, 1999; ISBN 3-446-17418-4.
48. Baldan, A. Adhesively-Bonded Joints and Repairs in Metallic Alloys, Polymers and Composite Materials: Adhesives, Adhesion Theories and Surface Pretreatment. *J. Mater. Sci.* **2004**, *39*, 1–49. [CrossRef]
49. Mandolfino, C.; Lertora, E.; Genna, S.; Leone, C.; Gambaro, C. Effect of Laser and Plasma Surface Cleaning on Mechanical Properties of Adhesive Bonded Joints. *Procedia CIRP* **2015**, *33*, 458–463. [CrossRef]
50. Boutar, Y.; Naïmi, S.; Mezlini, S.; Da Silva, L.F.M.; Hamdaoui, M.; Ben Sik Ali, M. Effect of Adhesive Thickness and Surface Roughness on the Shear Strength of Aluminium One-Component Polyurethane Adhesive Single-Lap Joints for Automotive Applications. *J. Adhes. Sci. Technol.* **2016**, *30*, 1913–1929. [CrossRef]
51. Gleich, D.M.; Van Tooren, M.J.L.; Beukers, A. Analysis and Evaluation of Bondline Thickness Effects on Failure Load in Adhesively Bonded Structures. *J. Adhes. Sci. Technol.* **2001**, *15*, 1091–1101. [CrossRef]
52. Lalehpour, A.; Janeteas, C.; Barari, A. Surface Roughness of FDM Parts after Post-Processing with Acetone Vapor Bath Smoothing Process. *Int. J. Adv. Manuf. Technol.* **2018**, *95*, 1505–1520. [CrossRef]
53. Mendelson, R.A. A Generalized Melt Viscosity-temperature Dependence for Styrene and Styrene-acrylonitrile Based Polymers. *Polym. Eng. Sci.* **1976**, *16*, 690–696. [CrossRef]

54. Rosenzweig, N.; Narkis, M. Sintering Rheology of Amorphous Polymers. *Polym. Eng. Sci.* **1981**, *21*, 1167–1170. [CrossRef]
55. Van Weeren, R.; Agarwala, M.; Jamalabad, V.R.; Bandyophadyay, A.; Vaidyanathan, R.; Langrana, N.; Safari, A.; Whalen, P.; Danforth, S.C.; Ballard, C. Quality of Parts Processed by Fused Deposition. In Proceedings of the 1995 International Solid Freeform Fabrication Symposium, Austin, TX, USA, 7–9 August 1995; Volume 6, pp. 314–321.
56. Kweon, J.H.; Jung, J.W.; Kim, T.H.; Choi, J.H.; Kim, D.H. Failure of Carbon Composite-to-Aluminum Joints with Combined Mechanical Fastening and Adhesive Bonding. *Compos. Struct.* **2006**, *75*, 192–198. [CrossRef]
57. Kim, K.S.; Yoo, J.S.; Yi, Y.M.; Kim, C.G. Failure Mode and Strength of Uni-Directional Composite Single Lap Bonded Joints with Different Bonding Methods. *Compos. Struct.* **2006**, *72*, 477–485. [CrossRef]
58. Mazumdar, S.K.; Mallick, P.K. Static and Fatigue Behavior of Adhesive Joints in SMC-SMC Composites. *Polym. Compos.* **1998**, *19*, 139–146. [CrossRef]
59. Objois, A.; Gilibert, Y.; Fargette, B. Theoretical and Experimental Analysis of the Scarf Joint Bonded Structure: Influence of the Adhesive Thickness on the Micro-Mechanical Behavior. *J. Adhes.* **1999**, *70*, 13–32. [CrossRef]
60. Fatimatuzahraa, A.W.; Farahaina, B.; Yusoff, W.A.Y. The Effect of Employing Different Raster Orientations on the Mechanical Properties and Microstructure of Fused Deposition Modeling Parts. In Proceedings of the 2011 IEEE Symposium on Business, Engineering and Industrial Applications ISBEIA, Langkawi, Malaysia, 25–28 September 2011; pp. 22–27.
61. Wu, W.; Geng, P.; Li, G.; Zhao, D.; Zhang, H.; Zhao, J. Influence of Layer Thickness and Raster Angle on the Mechanical Properties of 3D-Printed PEEK and a Comparative Mechanical Study between PEEK and ABS. *Materials* **2015**, *8*, 5834–5846. [CrossRef]
62. Tekinalp, H.L.; Kunc, V.; Velez-Garcia, G.M.; Duty, C.E.; Love, L.J.; Naskar, A.K.; Blue, C.A.; Ozcan, S. Highly Oriented Carbon Fiber-Polymer Composites via Additive Manufacturing. *Compos. Sci. Technol.* **2014**, *105*, 144–150. [CrossRef]
63. Tronvoll, S.A.; Welo, T.; Elverum, C.W. The Effects of Voids on Structural Properties of Fused Deposition Modelled Parts: A Probabilistic Approach. *Int. J. Adv. Manuf. Technol.* **2018**, *97*, 3607–3618. [CrossRef]
64. Lay, M.; Thajudin, N.L.N.; Hamid, Z.A.A.; Rusli, A.; Abdullah, M.K.; Shuib, R.K. Comparison of Physical and Mechanical Properties of PLA, ABS and Nylon 6 Fabricated Using Fused Deposition Modeling and Injection Molding. *Compos. Part B Eng.* **2019**, *176*, 107341. [CrossRef]